Preparation of Evaporation-Resistant Aqueous Microdroplet Arrays as a Model System for the Study of Molecular Order at the Liquid/Air Interface

Evelyn Meyer,[†,‡] Martin Mueller,[†] and Hans-Georg Braun*[,†,‡]

Leibniz Institute of Polymer Research Dresden, Hohe Strasse 6, D-01069 Dresden, Germany, and Max Bergmann Center of Biomaterials, Budapester Strasse 27, D-01069 Dresden, Germany

ABSTRACT Aqueous arrays of microdroplets typically sized between 2 and 10 μm were generated by microfluid contact printing and stabilized with respect to evaporation by incorporation of poly(ethylene oxide). The arrays are used as a model system for the study of structure formation at liquid/air or liquid/liquid interfaces. In particular, we demonstrated the self-organization of fatty acids with photopolymerizable diacetylene units (10,12-pentacosadiynoic acid) at the liquid/air interface of the microdroplets. Topochemical polymerization behavior of this compound and the autofluorescence property of the resulting polyconjugated polymer are appropriate features to prove the molecular order of the amphiphilic molecules at the interface.

KEYWORDS: poly(ethylene oxide) • microdroplet arrays • liquid interfaces • polydiacetylenes • microemulsion • soft lithography

INTRODUCTION

Small droplets are more and more used as microreactors for material syntheses (1, 2), for chemical syntheses of biofunctional molecules (3, 4) or as microanalytical devices (5, 6). The droplets may be generated in a microflow system as monodisperse droplets that are freely movable in a two-phase liquid/liquid system (water-in-oil or vice versa) (7). The droplet fluid/fluid interfaces are generally stabilized by surface-active compounds (8) and frequently functionalized with biofunctional molecular units by appropriate phospholipids, which self-assemble into mono- or bilayers (9). The interior space can be loaded with soluble reactants or even with single cells (10). For microanalytical investigations positional control of fluid phases becomes relevant and requires the immobilization of microdroplets in well-defined ordered arrays. The droplets should finally include biologically relevant molecular units as well as surface-active compounds. Droplet patterning can be done by various methods with specific advantages and disadvantages. Microdroplet patterning of aqueous droplets can be generated by water condensation from the vapor phase onto micropatterned surfaces with predefined areas of preferred wettability (11) or by surface-controlled dewetting on chemically (12) or topographically (13) structured surfaces. Often these water droplets will not contain any additional compounds. Droplet arrays patterned by inkjet deposition (14) can contain additional material, but the droplets and their included compounds are distributed over a large contact area because of droplet impact. Another method that has been used to obtain ordered arrays of polymer solutions on a surface is microfluid contact printing (μFCP) (15). μFCP is part of the soft-lithographic patterning techniques (16, 17). Although μFCP is only used as a tool for microdroplet generation in this paper and was described in detail elsewhere (15), its basic features, because they are relevant for experimental studies described here, will be briefly outlined.

A macroscopic droplet of a solution is deposited on the topographically structured surface of a poly(dimethylsiloxane) (PDMS) stamp. Excessive volume is blown under a N_2 flow and a residual liquid film ruptures because of the stamp topography, and single self-centered microdroplets (Figure 1A) are formed on each protrusion (hexagonal motif; Figure 1D) of the stamp. These droplets are transferred by stamping on a homogeneous surface with low spreading properties (Figure 1B,C). The process of microdroplet formation is strongly dependent on the wettability and the evaporation rate of the fluid on the PDMS stamp. While chloroform solutions with sufficiently low contact angle ($\theta_{\text{chloroform/PDMS}} \simeq 33°$) (18) coat the stamp and generate a thin film that decomposes in individual microdroplets during the evaporation process, aqueous solutions behave completely differently. Hydrophobicity of PDMS ($\theta_{\text{water/PDMS}} \simeq 115°$) in combination with its surface topography creates an ultrahydrophobic stamp surface that is nonwettable for water ($\theta_{\text{water/PDMS(structured)}} \simeq 145°$) (19). A macroscopic droplet on such a surface shrinks during evaporation without forming a thin film that could decompose into isolated microdroplets. Consequently, the generation and
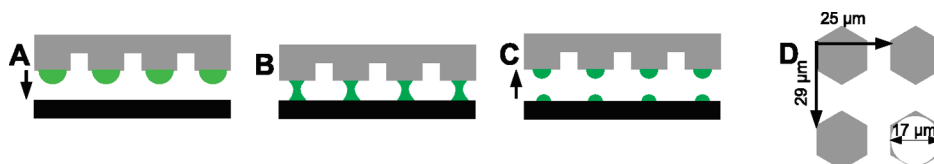
FIGURE 1. Scheme of the μFCP process (A−C) and geometrical motif of the PDMS stamp (D).

transfer of aqueous microdroplets by μFCP needs to overcome these problems, as will be shown in this paper.

Besides the problem of generating femtoliter-sized aqueous droplets by patterning techniques, solvent evaporation is a serious problem for the stability of the microdroplet arrays. Aqueous micrometer-sized droplets evaporate within a few seconds (20) either under shrinking with a constant contact angle (21) or with decreasing contact angle (22) when pinning at surface inhomogeneities occurs. This paper describes a new approach to preparing arrays of aqueous microdroplets in which further compounds can be transferred and which are stable with respect to evaporation. The stabilized microdroplet arrays are used to study structure formation at liquid/liquid or liquid/air interfaces in femtoliter dimensions.

In order to characterize the molecular order at the droplet interface, an appropriate amphiphile with diacetylenic molecular units was chosen that indicates the well-ordered state by the topochemical reactivity (23) and autofluorescence of the polymerized product.

EXPERIMENTAL SECTION

Poly(ethylene oxide) (PEO; $M_n \sim 2000$ g/mol) was obtained from Polymer Standards. 1-Hydroxycyclohexyl phenyl ketone (Irgacure 184), poly(ethylene glycol diacrylate), trimethylchlorosilane, octadecylmercaptan, chloroform, and hexadecane (analytical grade) came from Sigma. Solvents were used without further purification. Gold granulate (99.99 grade) was obtained from Saxonia Metals, Freiberg, Germany. 1,2-Dipalmitoyl-*sn*-glycero-3-phosphoethanolamine-*N*-(7-nitro-2,1-benzoxadiazol-4-yl) ammonium salt (16:0 NBD-PE) was purchased from Invitrogen. 12,8-Pentacosadiynoic acid (PCDA; CAS 66990-32-7) was obtained from Alfa Aesa. Elastomeric PDMS stamps (Sylgard 184; Dow Chemical) were prepared from silicon-etched master structures according to standard procedures (17). Prior to replication, the silicon masters were carefully cleaned and the surface was treated with trimethylchlorosilane to avoid irreversible sticking of PDMS to the silicon surface. For μFCP of a pure PEO solution, PDMS stamps (Figure 1) were inked with PEO/chloroform solutions of typically 1 % (w/w) poly(ethylene oxide diacrylate) microdroplets prepared with a 3 % poly(ethylene oxide diacrylate)/Irgacure 184 [100:1 (w/w)]/chloroform solution. For photo-cross-linking, the droplets were irradiated with UV light ($\lambda = 365$ nm) of an ordinary laboratory UV lamp under a N_2 atmosphere for about 3 min.

Microdroplets were printed onto hydrophobized gold layers. Prior to gold coating, a cleaned microscopic cover glass is coated with a 2−3 nm chromium layer as an adhesion promoter followed by a 10 nm gold layer, which is transparent enough for bright-field microscopy in transmission. Evaporation of chromium or gold was done in a high-vacuum coating unit (Leybold Univex 300) equipped with two thermal evaporators. Metal evaporation was performed in a chamber vacuum of 10^{-5} mbar and with typical evaporation rates of 1.0 nm/s.

For surface hydrophobization, the gold surface was treated for 15 min with 2 mmol of an octadecylmercaptan/ethanol solution to avoid spreading of the hydrophilic microdroplets.

Microprinted droplets were inspected by a Zeiss Axiovert 135 inverse light microscope. For fluorescence imaging, an HBO100 lamp and an appropriate filter set (excitation, $\lambda = 450-490$ nm; emission LP, $\lambda = 520$ nm) were used. Fluorescence images were recorded with a cooled 12-bit CCD camera (SPOT Xplorer 1.4, MP Diagnostics Inc.). For image processing, either Metamorph or ImageJ Software (http://rsb.info.nih.gov/ij/) was used. Scanning electron microscopy investigations were done with a Zeiss DSM 982 Gemini scanning electron microscope operating at low-voltage imaging conditions (1 keV).

In situ Fourier transform infrared (FTIR) experiments regarding solvent exchange (chloroform vs water) were done with a FTIR spectrometer (Bruker Equinox 55) equipped with an attenuated total reflectance (ATR) cell. By multiple fluid contact printing of a PEO solution in chloroform, an area of 10 mm × 10 mm on a Ge substrate was coated by microdroplet arrays. The ATR setup was part of an in-house-built in situ chamber that allowed control of the gas atmosphere around the sample.

RESULTS AND DISCUSSION

Microdroplet Generation and Droplet Properties. The aim of our present experiments focuses on the preparation of *aqueous* microdroplet arrays. As mentioned in the Introduction, the partitioning of a macroscopic water droplet on the protrusions of the PDMS stamp and therefore the transfer of individual microdroplets on a substrate are not realizable. However, μFCP experiments with hydrophilic PEO/chloroform solutions showed a remarkable effect. As observed for a number of organic solvents, the PEO/chloroform solution decomposes into a set of microdroplets centered on each protrusion of the PDMS stamp. Generally, the volatile solvent evaporates and leaves an array of well-ordered solidified polymer residues on the stamp. However, in the case of PEO/chloroform, the droplets are stable with respect to solvent evaporation and remain almost an unlimited liquid under ordinary atmospheric humidity conditions in the laboratory. As demonstrated by Figure 2, the droplet array can be transferred from the stamp to a substrate, again keeping the liquid state. It is most unlikely that the PEO solution still contains the volatile chloroform, but it is much more probable that chloroform has exchanged against water, which is absorbed from the atmosphere. Because of the well-known affinity of PEO segments to water molecules, it can be assumed that as soon as chloroform evaporates PEO segments immediately accumulate water from the surrounding atmosphere (24, 25).

The number of water molecules interacting with one ethylene oxide segment through hydrogen bonding is still under discussion, and numbers vary between 0.5 (26) and 3 water molecules per ethylene oxide segment (27). In particular, it was demonstrated by NMR measurement (26) that at low water content hydrogen bonding between water molecules and ethylene oxide segments results in a strong bridging of the PEO chains, reducing the mobility of both

FIGURE 2. Reflective light microscope image of fluid droplets transferred onto a hydrophobized gold surface (scale bar = 25 μm).
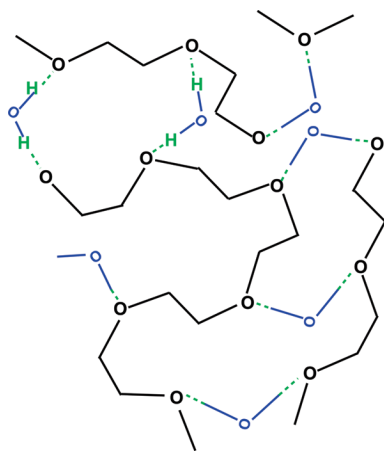

FIGURE 3. Schematic hydrogen-bonding network in a concentrated PEO/water system (26).

the ethylene oxide segments and the water molecules. The internal structure of water/PEO microdroplets might be best described as shown schematically in Figure 3.

We observe that only microdroplets smaller than ca. 10 μm remain in a liquidlike state, while in larger-sized droplets, the PEO phase tends to solidify by crystallization. The reason that microsized droplets remain liquid may result from their high specific surface area, which causes higher water incorporation compared to larger droplets. Additionally, micrometer-sized droplets do not crystallize because of the lack of nuclei necessary for heterogeneous nucleation, and finally the strong interaction between ethylene oxide segments and water molecules will stabilize the PEO/water association.

The assumption of the chloroform/water exchange is supported by the observation that PEO-containing microdroplets transferred into a scanning electron microscope solidify under high-vacuum conditions ($p \sim 10^{-5}$ Torr) and become liquid again under an ordinary laboratory atmosphere. As SEM images demonstrate, microdroplets form the shape of a spherical cap (Figure 4), which is typical for a solidified noncrystalline droplet and which is clearly distinguishable from microdroplets crystallized in stacks of lamellar PEO crystals (Figure 5) (28). Only the solidified noncrys-
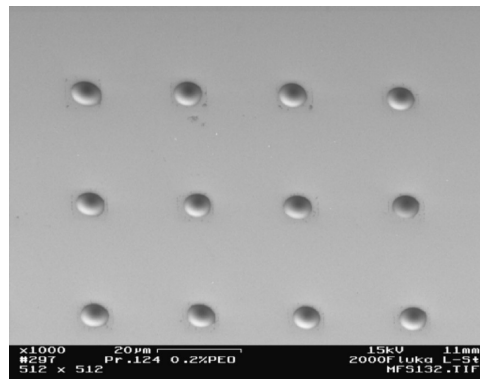

FIGURE 4. SEM image of amorphous solidified PEO droplets demonstrating the initial spherical shape of the microdroplets.
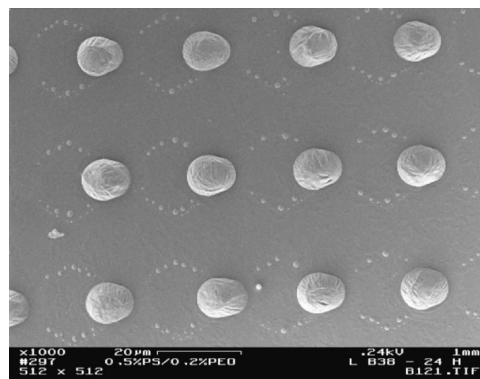

FIGURE 5. SEM image of crystallized PEO microdroplets.

talline PEO phase rehydrates after removal from the high vacuum of the scanning electron microscope, resulting in liquid microdroplets. In contrast, larger PEO phases that have been crystallized keep their multilamellar structure and do not rehydrate.

In order to verify the solvent exchange of chloroform versus water, a number of microdroplet arrays is transferred to a Ge-ATR plate and investigated by ATR-FTIR spectroscopy. In the ATR-FTIR spectra for microdroplet arrays as-prepared (A) and for modified samples (B and C) (Figure 6), diagnostic IR bands at around 3400−3200 and 1650 cm^{-1} could be identified that can be assigned to the n(OH) stretching and d(OH) bending vibrations of water. Hence, one can conclude that the as-prepared PEO arrays have a considerable amount of water. To check if water from other locations like the bare regions of the Ge-internal reflection element (IRE) could contribute to the water bands, the sample was exposed to a H_2O gaseous atmosphere, which resulted in a slight increase of these band intensities originating from the increasing water content. Moreover, after drying of sample B, the band intensities assigned to the water bands again decreased, but a certain amount of water remained, which should be attributed to the PEO moieties. In addition, the band at around 1100 cm^{-1}, which can be assigned to the n(C−O−C) band of PEO showed a slight downshift of around 5 cm^{-1} for the hydrated sample in comparison to the dry one, which proves that water predominantly interacts with the PEO patches and not with the bare regions of GE-IRE.
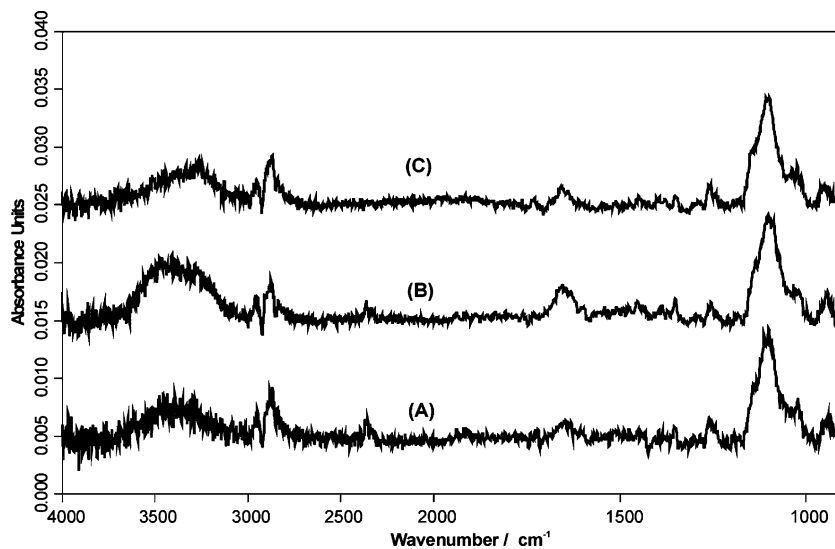
FIGURE 6. ATR-FTIR spectra of PEO microdroplet arrays on Ge-IRE: (A) PEO sample as-prepared; (B) PEO sample in contact with a humid N$_2$/H$_2$O gas stream; (C) sample B after drying in a dry N$_2$ stream.
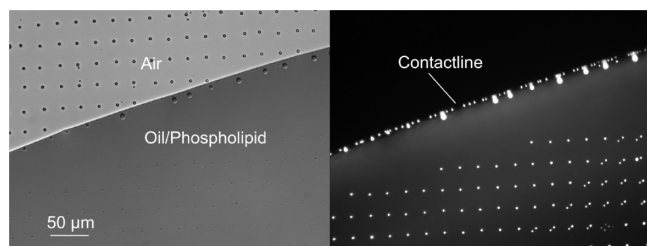

FIGURE 7. Transmission light microscope image of a microdroplet array partially covered by a fluorescent phospholipid (16:0 NBA-PE) that is dissolved in the oil phase (hexadecane) (left). Corresponding fluorescent image (same position) indicating the nonfluorescent area outside the oil phase and the fluorescent phospholipids decorating the water/oil interface of water microdroplets (right).

In order to support further the idea of the chloroform/water exchange, the PEO droplets were covered with an oil phase (hexadecane) of several 100 μm thickness that contains a fluorescent phospholipid (16:0 NBD-PE). The amphiphilic phospholipid molecules should become assembled at the water/oil interface. The fluorescence imaging clearly reveals that the hydrophilic head groups of the phospholipid dyes are concentrated around the PEO microdroplets, which also indicates the presence of water within the droplets (Figure 7). This figure also shows that the periodic positions of the droplets defined by the stamping process are preserved after being covered by the oil phase. Only some droplets near the three-phase contact line of the covered oil phase are obviously moved to the contact line. The transport of these particles results from the enhanced internal flow near the three-phase contact line within an evaporating drop (29).

In order to stabilize the liquid PEO microdroplet array with respect to shear flow, PEO is replaced by photo-cross-linkable poly(ethylene oxide diacrylate) with small amounts of photoinitiator (Irgacure). After photoirradiation ($\lambda = 365$ nm) under a N$_2$ atmosphere, cross-linked poly(ethylene oxide diacrylate) microdroplets that also contain water are generated. Coverage of these aqueous PEO hydrogel arrays with an amphiphilic phospholipid/oil solution yields results

similar to those demonstrated in Figure 7. The aqueous PEO gel phase in contact with a phospholipid-containing oil assembles the surface-active molecules at the water/oil interfaces, and the lipid layer finally embeds the PEO gel microdroplets. Contrary to the pure PEO microdroplets, the PEO hydrogel droplets are immobilized at the surface and droplet movements due to flow effects are not observed. The poly(ethylene oxide diacrylate) arrays are stable with respect to water and alcohol treatment and allow therefore covering of *aqueous* systems *on aqueous* microdroplet arrays and, consequently, the exchange of water-soluble compounds from the water-containing PEO gel phase into a surrounding water phase or in reverse order without shifting of individual droplets or destruction of the microdroplet arrays.

Interfacial Design with Phospholipids and Topochemical Polymerizable Diacetylenes. As was already described for poly(ethylene oxide diacrylate) transfer by μFCP, other chemical compounds that are soluble in chloroform such as the photoinitiator can be transferred into the aqueous PEO microdroplet phase and can be used for chemical reactions inside the microdroplets. In particular, phospholipids or photoreactive fatty acids were added to the PEO solution in chloroform in order to engineer aqueous/air or aqueous/oil interfaces.

Figure 8I shows an aqueous PEO microdroplet array in which the fluorescent lipid 16:0 NBD-PE has been dissolved in the PEO/chloroform system used for μFCP. After transfer and chloroform/water exchange, phospholipid molecules are assembled at the water/air interface, as shown in Figure 8II. Whether the fluorescent lipid molecules are in a disordered state, as indicated in Figure 8II, or whether they form a closed-packed layer similar to the compressed state on a film balance is not yet clear from the observations.

Cooling of the system from the initial state [Figure 8III (left)] below the dew point causes an increase in the aqueous droplet size because of water condensation from the surrounding atmosphere [Figure 8III (right)]. A remarkable observation demonstrated in Figure 8III (right) shows an
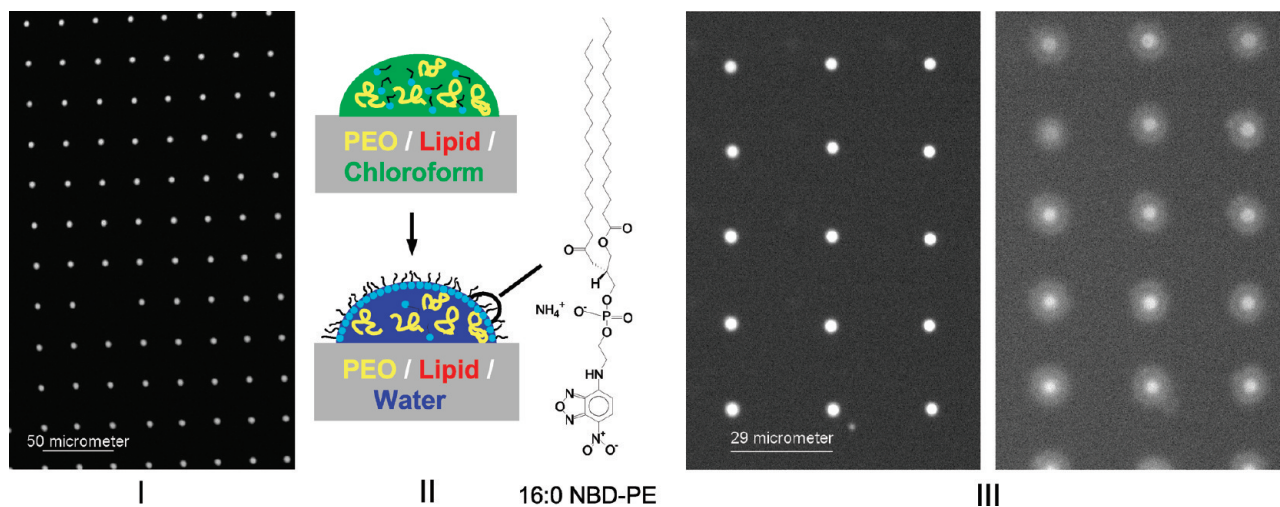
FIGURE 8. Fluorescence optical micrographs of a microarray of PEO-stabilized aqueous droplets with a fluorescent phospholipid at the liquid/air interface (I and II). The sample before and after additional water condensation from air (III).
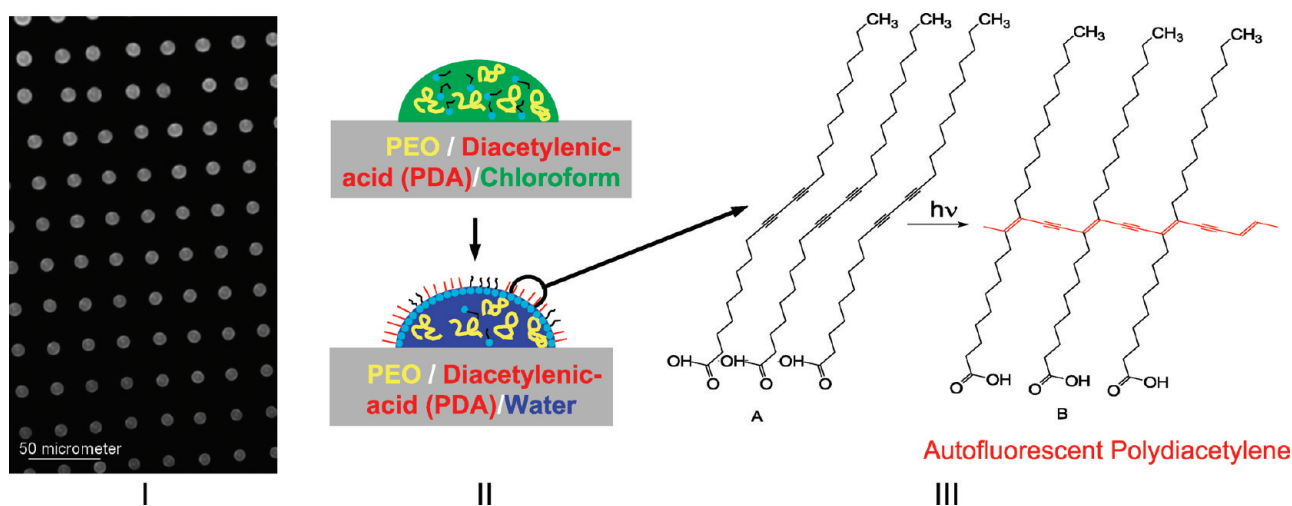

FIGURE 9. Fluorescent polydiacetylene interfacial layer (I and II) after topochemical polymerization of ordered PCDA domains (III).

enhanced fluorescent intensity in the center of the droplet instead of a homogeneous fluorescence distribution inside the enlarged microdroplet. We assume that indeed the core of the microdroplet representing the original PEO/water system is strongly hydrogen-bonded, as was already discussed, whereas the outer coating of the droplet is the condensed water. Most of the lipid molecules remain in contact with the PEO-rich core because of the strong PEO/lipid interaction, and therefore complete equilibration of the lipid concentration is inhibited.

In order to prove the interfacial molecular order of surface-active molecules at the liquid/air interface without sophisticated analytical equipment, we were looking for appropriate molecules that can indicate the state of order by their peculiar properties. As an indicator for molecular order, we used the topochemical reactivity of diacetylenes. The local order is indicated by the autofluorescence property of the polymerized reaction product (polydiacetylene). Our experiments are based on the interfacial behavior of the amphiphilic molecule 10,12-pentacosadiynoic acid (10,12-PCDA). PCDA is known to undergo a topochemical photopolymerization reaction (30, 31), in which adjacent triple

bonds of diacetylenic monomers react to build the polyconjugated polydiacetylene chain (Figure 9III). According to the topochemical reaction principles (23, 32), the reaction occurs only if the participating chemical reaction centers are within an ordered state that has to be preserved during the reaction. Studies on the polymerization behavior of 10,12-PCDA molecules at the water/air interface of a film balance (33) demonstrated the reactivity of the molecules in relation to their interfacial order. The polymerized molecules are known to exhibit a strong autofluorescence after thermally or mechanically induced stresses that result in a conformational change of the polyconjugated polydiacetylene backbone (34, 35). Consequently, the observation of autofluorescence in the system is analytical proof for the ordered state of the reacting PCDA molecules at the water/air interface. Figure 9I shows the fluorescence image of a microdroplet array in which 10,12-PCDA molecules were added to the chloroform/PEO solution. After exchange of chloroform against water, these amphiphilic diacetylene monomers are self-assembled at the microdroplet water/air interface (Figure 9II). The molecular packing at the interface must have been appropriate for the topochemical polymerization

process, which was initiated by UV irradiation and which finally, after stress or temperature treatment ($T = 80$ °C), resulted in the autofluorescent form of the polyconjugated polydiacetylene structure (Figure 9III), which commonly is referred to as the "red" phase. Nevertheless, we are aware that the appearance of fluorescent PCDA does not necessarily imply a homogeneous membrane structure but can also arise from locally ordered and therefore polymerizable domains at the droplet interface (Figure 9III). In addition, the topochemical conversion of PCDA at the microdroplet interface indicates the presence of molecular order between adjacent diacetylene entities, but it does not allow for one to decide whether the molecules are within a single-layer or multilayer structure.

The mechanosensitivity of the fluorescence (36) is of increasing interest for the preparation of sensing membrane systems (37−39) and has successfully been used to prepare bacterial (40) or viral (41) sensing liposomes.

CONCLUSIONS

In this article, we demonstrate the preparation of micropatterned arrays of aqueous microdroplets by μFCP. In general, the superhydrophobic behavior of the PDMS stamp prevents contact printing of pure water. In order to overcome this problem, we used a PEO/chloroform solution to wet a patterned stamp surface and to achieve a distribution of individual droplets on the stamp protrusions during the chloroform evaporation process. Strong interaction of PEO segments with water molecules favors the adsorption of water and the formation of water droplets on the protrusions of the stamp. The droplets can be transferred by μFCP onto a surface. PEO in the aqueous microdroplets guarantees droplet stability with respect to evaporation at common laboratory humidity conditions. This behavior is only observed in microsized droplets. Further chemical compounds such as amphiphilic molecules that typically participate in the membrane formation of emulsions or vesicles can be included in the aqueous phase.

For the study of structure formation at interfaces, we used 10,12-PCDA diacetylenic amphiphiles to characterize the ordered state within the liquid/air interface, taking advantage of the topochemical reaction path and the autofluorescence property of the polyconjugated polymer chains for analytical proof.

The integration of chloroform-soluble compounds into the aqueous phase and, in particular, the possibility of generating membrane systems around the micropatterned liquid aqueous phase offer a great potential for further use as microreactors. Stable aqueous microdroplet arrays with sensing and functional interfaces can be seen as a great chance for the future preparation of addressable microreactors in material synthesis and for biofunctional applications.

REFERENCES AND NOTES

(1) Rondeau, E.; Cooper-White, J. J. *Langmuir* **2008**, *24*, 6937–6945.
(2) Su, Y. F.; Kim, H.; Kovenklioglu, S.; Lee, W. Y. *J. Solid State Chem.* **2007**, *180*, 2625–2629.
(3) Taly, V.; Kelly, B. T.; Griffiths, A. D. *ChemBioChem* **2007**, *8*, 263–272.
(4) Kelly, B. T.; Baret, J. C.; Taly, V.; Griffiths, A. D. *Chem. Commun.* **2007**, 1773–1788.
(5) Engl, W.; Tachibana, M.; Colin, A.; Panizza, P. *Chem. Eng. Sci.* **2008**, *63*, 1692–1695.
(6) Laval, P.; Salmon, J. B.; Joanicot, M. *J. Cryst. Growth* **2007**, *303*, 622–628.
(7) Teh, S. Y.; Lin, R.; Hung, L. H.; Lee, A. P. *Lab Chip* **2008**, *8*, 198–220.
(8) Hase, M.; Yamada, A.; Hamada, T.; Baigl, D.; Yoshikawa, K. *Langmuir* **2007**, *23*, 348–352.
(9) Holden, M. A.; Needham, D.; Bayley, H. *J. Am. Chem. Soc.* **2007**, *129*, 8650–8655.
(10) Huebner, A.; Srisa-Art, M.; Holt, D.; Abell, C.; Hollfelder, F.; Demello, A. J.; Edel, J. B. *Chem. Commun.* **2007**, 1218–1220.
(11) Drelich, J.; Miller, J. D.; Kumar, A.; Whitesides, G. M. *Colloids Surf., A* **1994**, *93*, 1–13.
(12) Biebuyck, H. A.; Whitesides, G. M. *Langmuir* **1994**, *10*, 2790–2793.
(13) Jackman, R. J.; Duffy, D. C.; Ostuni, E.; Willmore, N. D.; Whitesides, G. M. *Anal. Chem.* **1998**, *70*, 2280–2287.
(14) de Gans, B. J.; Duineveld, P. C.; Schubert, U. S. *Adv. Mater.* **2004**, *16*, 203–213.
(15) Wang, M. T.; Braun, H. G.; Kratzmuller, T.; Meyer, E. *Adv. Mater.* **2001**, *13*, 1312–1317.
(16) Xia, Y. N.; Whitesides, G. M. *Annu. Rev. Mater. Sci.* **1998**, *28*, 153–184.
(17) Xia, Y.; Whitesides, G. *Angew. Chem., Int. Ed.* **1998**, *37*, 550–575.
(18) Takakuwa, A.; Azumi, R. *Jpn. J. Appl. Phys.* **2008**, *47*, 1115–1118.
(19) Manca, M.; Cortese, B.; Viola, I.; Arico, A. S.; Cingolani, R.; Gigli, G. *Langmuir* **2008**, *24*, 1833–1843.
(20) Birdi, K. S.; Vu, D. T.; Winter, A. *J. Phys. Chem.* **1989**, *93*, 3702–3703.
(21) Erbil, H. Y.; McHale, G.; Newton, M. I. *Langmuir* **2002**, *18*, 2636–2641.
(22) Yu, H. Z.; Soolaman, D. M.; Rowe, A. W.; Banks, J. T. *ChemPhysChem* **2004**, *5*, 1035–1038.
(23) Curtis, S. M.; Le, N.; Nguyen, T.; Xi, O. Y.; Tran, T.; Fowler, F. W.; Lauher, J. W. *Supramol. Chem.* **2005**, *17*, 31–36.
(24) Richartz, T.; Galle, J.; Klose, G. *Chem. Phys. Lett.* **1997**, *271*, 79–83.
(25) Hey, M. J.; Ilett, S. M. *J. Chem. Soc., Faraday Trans.* **1991**, *87*, 3671–3675.
(26) Lusse, S.; Arnold, K. *Macromolecules* **1996**, *29*, 4251–4257.
(27) Hammouda, B.; Ho, D. L.; Kline, S. *Macromolecules* **2004**, *37*, 6932–6937.
(28) Meyer, E.; Braun, H. G. *J. Phys. C: Condens. Matter* **2005**, *17*, S623–S635.
(29) Hu, H.; Larson, R. G. *Langmuir* **2005**, *21*, 3963–3971.
(30) Lieser, G.; Tieke, B.; Wegner, G. *Thin Solid Films* **1980**, *68*, 77–90.
(31) Tieke, B. *Adv. Polym. Sci.* **1985**, *71*, 79–151.
(32) Wegner, G. *Makromol. Chem.* **1972**, *154*, 35.
(33) Mino, N.; Tamura, H.; Ogawa, K. *Langmuir* **1992**, *8*, 594–598.
(34) Barisien, T.; Legrand, L.; Weiser, G.; Deschamps, J.; Balog, M.; Boury, B.; Dutremez, S. G.; Schott, M. *Chem. Phys. Lett.* **2007**, *444*, 309–313.
(35) Schott, M. *J. Phys. Chem. B* **2006**, *110*, 15864–15868.
(36) Carpick, R. W.; Sasaki, D. Y.; Burns, A. R. *Langmuir* **2000**, *16*, 1270–1278.
(37) Kew, S. J.; Hall, E. A. H. *Anal. Chem.* **2006**, *78*, 2231–2238.
(38) Lee, S. W.; Kang, C. D.; Yang, D. H.; Lee, J. S.; Kim, J. M.; Ahn, D. J.; Sim, S. J. *Adv. Funct. Mater.* **2007**, *17*, 2038–2044.
(39) Reppy, M. A.; Pindzola, B. A. *Chem. Commun.* **2007**, 4317–4338.
(40) Silbert, L.; Ben Shlush, I.; Israel, E.; Porgador, A.; Kolusheva, S.; Jelinek, R. *Appl. Environ. Microbiol.* **2006**, *72*, 7339–7344.
(41) Orynbayeva, Z.; Kolusheva, S.; Groysman, N.; Gavrielov, N.; Lobel, L.; Jelinek, R. *J. Virol.* **2007**, *81*, 1140–1147.

AM900249W